Atmos. Chem. Phys. Discuss., 13, 2877–2912, 2013
www.atmos-chem-phys-discuss.net/13/2877/2013/
doi:10.5194/acpd-13-2877-2013

Atmospheric Chemistry and Physics Discussions

Aircraft measurements of gases pollutants and particles during CAREBeijing-2008: distributions, characteristics and influencing factors

W. Zhang[1,2], T. Zhu[2], W. Yang[1], Z. Bai[1], Y. L. Sun[3], Y. Xu[1], and B. Yin[1]

[1]State Key Laboratory of Environmental Criteria and Risk Assessment, Chinese Research Academy of Environmental Sciences, Beijing 100012, China
[2]State Key Joint Laboratory of Environmental Simulation and Pollution Control, College of Environmental Sciences and Engineering, Peking University, Beijing 100871, China
[3]State Key Laboratory of Atmospheric Boundary Layer Physics and Atmospheric Chemistry, Institute of Atmospheric Physics, Chinese Academy of Sciences, Beijing 100029, China

Received: 16 December 2012 – Accepted: 8 January 2013 – Published: 28 January 2013

Correspondence to: W. Zhang (zhangwj@craes.org.cn) and Z. Bai(baizp@craes.org.cn)

Published by Copernicus Publications on behalf of the European Geosciences Union.

Abstract

Measurements of gaseous pollutants, including ozone (O_3), sulfur dioxide (SO_2), nitrogen oxides (NO_x = NO + NO_2), carbon monoxide (CO), particle number concentrations (5.6–560 nm and 0.47–30 µm), and meteorological parameters (T, RH, P) were conducted during the Program of Campaigns of Air Quality Research in Beijing and Surrounding Region (CAREBeijing) from 27 August through 13 October 2008. The data of total 18 flights (70 h flight time) from the ground to 2100 m were obtained by a Yun-12 aircraft in the southern surrounded areas of Beijing (38° N–40° N, 114° E–118° E). This measurement was to characterize the regional variation of air pollution during and after the Olympics of 2008, the impacts of different transport direction and possible influencing factors. Results suggested that four different groups of transport sources influenced the pollution level of pollutants with the consideration of the backward trajectory analysis, including: (1) the pollutant transport of the southern direction with higher pollutants level; (2) the cleaner long-range transport of the northern or northwestern direction with lower pollutants level; (3) the transport from the eastern direction with characteristics of sea sources, i.e. middle level of gases pollutants and higher particle concentration; (4) the transport of mixing directions, i.e. lower altitudes from the pollutant transport direction or local pollution but higher altitudes from the clean transport direction. Additionally, the relatively long-lived CO was shown to be a possible transport tracer of long-range transport of northwestern direction especially on the higher altitudes. Three factors influenced the size distribution of particles, i.e. air mass transport direction, ground source emissions and meteorological influences were also discussed.

1 Introduction

As the host of the 2008 Olympic Games, the air quality of Beijing has been paid worldwide attention to. In China, the Beijing and National governments have been introducing many new pollution control measures to reduce local emissions in Beijing (Beijing

ACPD
13, 2877–2912, 2013

Organizing Committee of the XXIX Olympic Games, 2005; Streets et al., 2007). Many studies have been conducted to the air pollution in Beijing and surround areas.

While, the air pollution in Beijing is regional in nature and not attributable to local sources. An international field campaign "Campaigns of Air Quality Research in Beijing and Surrounding Region 2006" (CAREBeijing-2006) was conducted in summer 2006. The publications of CAREBeijing-2006 studies confirmed that the air pollution in Beijing was a regional problem on a scale of up to 1000 km (Garland et al., 2009; Jung et al., 2009; Matsui et al., 2009), and high pollution periods were usually associated with air masses from the south transport directions (Takegawa et al., 2009; van Pinxteren et al., 2009; Yue et al., 2009). Another research estimated that 34 % of $PM_{2.5}$ on average and 35 ~ 60 % of ozone during high ozone episodes were attributed to sources outside of Beijing, based on the Models-3/CMAQ model simulation results. They also found that the neighboring Hebei province could contribute 50–70 % of Beijing's $PM_{2.5}$ and 20–30 % of ozone contributions during sustained wind flow from the south (Streets et al., 2007).

However, fewer researches on large-scale aircraft measurement of regional pollution were reported during the summer periods in Beijing and surrounding areas. Aircraft provide a horizontally and vertically mobile sampling platform. The horizontal mobility allows for deployment to specific areas of interest, while the vertical mobility provides insight into boundary layer dynamics, and allows for measurement representative of a larger area (Taubman et al., 2006). Many projects and correspondingly a series of aircraft field campaigns were carried out in China. The Asia Pacific Regional Aerosol Characterization Experiment (ACE-Asia, Kawamura et al., 2003; Huebert et al., 2004; Simoneit et al., 2004) made the aircraft measurements on organic carbon/elemental carbon and organic aerosols over the Yellow Sea and East China Sea, the outflow region of Chinese aerosols, as well as the spatial and vertical distributions of organic aerosols over coastal and inland China (Wang, et al., 2007). An international project of Atmospheric Brown Clouds-East Asian Regional Experiment (ABC, Wang et al., 2005, 2008a) have been conducted in China since early 1990s, many national projects such

ACPD
13, 2877–2912, 2013

as natural science foundation have also supported many aircraft field campaigns. The size distribution of airborne particles over eastern coastal areas (Wang et al., 2005), vertical ultrafine particles profiles over Northern China coastal areas during dust storms (Wang et al., 2008a), and gaseous and particulate pollutants over Pearl River Delta (Wang et al., 2008b) were reported. Another aircraft observation from the Transport and Chemical Evolution over the Pacific (TRACE-P, Tu et al., 2003) showed substantial concentrations of SO_2 over Pacific downwind of China (Dickerson et al., 2007). Another Chinese/American joint project of EAST-AIRE (the East Asian Study of Tropospheric Aerosols-an International Regional Experiment, Li et al., 2007) investigated the vertical distribution of pollutants and dust over East Asia from eight flights under a variety of weather conditions in northeastern China centered over Shenyang, a large industrial city 650 km northeast of Beijing, shedding light on the mechanisms of long-range pollutant transport out of east Asia (Li et al., 2007; Dickerson et al., 2007).

The aircraft measurements mentioned above have been conducted over coastal areas, or northwestern China on a regional level. There are few measurements over Beijing region, except a case study of the aerosols (Zhang et al., 2006) and an in-situ aircraft measurements over 2005–2006 (Zhang et al., 2009) before the control measurements for the Olympic Games. "Campaigns of Air Quality Research in Beijing and Surrounding Region-2008 (CAREBeijing-2008)" was a follow-up international field campaign of CAREBeijing-2006 led by Peking University, which aimed at characterizing the air quality during the 2008 Beijing Olympic Games (Huang et al., 2010). As part of CAREBeijing-2008, this paper summarizes the regional variation of gaseous pollutants and particles during and after the Olympics of 2008 by 18 flights of aircraft measurements, and discussed the possible impacts of different transport direction and influencing factors.

ACPD
13, 2877–2912, 2013

2 Experimental

2.1 Flight information

A Yun-12 aircraft with a cruising speed of about 180 km h^{-1} was used for all the flights. The aircraft measurements were conducted from 27 August to 13 October over the Beijing surrounding areas, i.e. the area to the south of Beijing in Hebei Province and Tianjin. Total three different flight routes (18 flights) with 70 h flights were made during this campaign, as shown in Fig. 1. More detailed flight information is summarized in Table 1.

All the flights were conducted in "linear" pattern between different sites. Along flight route 1, 10 flights were carried out between Zaojiacheng (ZJC, 39°17′ N, 117°27′ E) and Anci (AC, 39°31′ N, 116°42′ E) cities at three different altitudes of 2100 m, 900 m, and 600 m. For the flight route 2, 4 fights were carried out between Anci (AC, 39°31′ N, 116°42′ E) and Zhuozhou (ZZ, 39°29′ N, 115°58′ E) cities at three different altitudes of 2100 m, 900 m, and 600 m. All the flights of route 1 and 2 at different altitudes were conducted for at least 2 ∼ 3 times between these different sites. The flight route 3 includes 5 different cities, and the flights were conducted in the sequence of Zaojiacheng, Anci, Zhuozhou, Baoding (BD, 38°52′ N, 115°28′ E), and Shijiazhuang (SJZ, 38°3′ N, 114°31′ E), with the "linear" pattern flight from one city to the next one.

The flights covered most southern areas to Beijing. The aircraft takes off at Binhai Airport (BH, 39°8′ N, 117°21′ E) in Tianjin, and then fly covered ZJC in Tianjin, AC, ZZ, BD, and SJZ in Hebei Province. Most of the cities are located to the south side of Beijing. BH and ZJ belong to Tianjin, and the other four cities belong to Hebei Province. As the biggest power suppliers for the megacities of Beijing and Tianjin, many electric power plants are located in Hebei province. About 20 large electric power plants were located in this region. Additionally, several inter-state highways crossed along the flight routes. There are also high density of small towns and villages in this region. As a result, the local emissions of air pollutants from automobiles, coal burning, and area and point sources are intensive.

ACPD
13, 2877–2912, 2013

2.2 Instrumentation on the aircraft

Several commercial instruments were mounted on the aircraft to measure the concentration of O_3, NO_x ($NO + NO_2$), CO, SO_2, CO_2, and particle number concentrations of condensation nucleus (CN). Ozone (O_3) was measured by a commercial UV photometric analyzer (Thermo Environmental Instruments Inc. (TECO), model TE/49i) with a detection limit of 0.5 ppbV and a precision of ±1 ppbV. It operates on the principle that O_3 molecules absorb UV light at a wavelength of 254 nm, and the degree to which the UV light absorbed is directly related to the ozone concentration. During each flight, the measuring range was set from 0.5 to 200 ppbV with the automatic temperature and pressure correction. $NO–NO_2–NO_x$ was monitored with an O_3-chemiluminescent trace level analyzer (TECO, model TE/42i) with a detection limit of 0.4 ppbV. It is operated on the principle that nitric oxide (NO) and ozone (O_3) react to produce a characteristic luminescence with an intensity of linearly proportional to the NO concentration. The NO and NO_x concentrations calculated in the NO and NO_x modes are stored in memory, and the difference between the concentrations is used to calculate the NO_2 concentration. Sulfur dioxide (SO_2) measurement was used a pulsed ultraviolet (UV) fluorescence analyzer (TECO, model TE/43i), based on the principle that SO_2 molecules absorb UV light and become excited at one wavelength, then decay to a lower energy state emitting UV light at a different wavelength. The detection limit of the analyzer is 0.5 ppbV for 5-min integration with a precision of 0.2 ppbV. Carbon monoxide (CO) was detected with a gas filter correlation CO Analyzer (TECO, model TE/48i), and is operated on the principle that carbon monoxide (CO) absorbs infrared radiation at a wavelength of 4.6 microns, using an internally stored calibration curve to accurately linearize the instrument output.

The number concentrations were measured with a condensation nuclei counter (CNC, TSI Corporation, USA, Model 3020). This device draws in air through a sample pipe situated in the aircraft, and saturates it with n-butanol. The level of saturation is maintained so that only the heterogeneous condensation occurs onto the small

ACPD
13, 2877–2912, 2013

particles within the air samples. Butanol droplets are subsequently counted by measurement of scattering of laser light. The size range for the instrument to measure is about 3 ~ 1000 nm, and the particles counted from 0.01 ~ 9.99 × 10^4 particles cm^{-3}.

Ultrafine particles concentration was measured with engine exhaust particle sizer spectrometer (EEPS) (TSI Corporation, USA, model 3090). It can measure the number concentration of particles ranging from 5.6 to 560 nm with 32 channels at 10 Hz frequency (TSI, 2013). According to the information provided by TSI, this instrument is not sensitive to pressure below the altitude of 3000 m (Wang et al., 2005, 2007, 2008; TSI, 2006). Size resolved particles number concentrations of $PM_{0.5}$ (particles with sizes less than 0.5 µm) were calculated as the sum of the number concentration of all channels.

Fine and coarse particles (0.47 ~ 30 µm) were used with the TSI Aerodynamic Particle Sizer Spectrometer (APS) (TSI Corporation, USA, model 3310) to sample particle size distributions. It uses 57 channels and gives number size distribution automatically. The surface and mass size distribution are calculated on the assumption that sampled particles have the same sedimentation rate as global particles of the density of 1 g cm^{-3} with the same diameters (Wang et al., 2005).

To keep constant flow rate and sampling pressure, a dome was adopted to introduce air into sampling tube. All the instruments were calibrated before the field campaign by injecting a span gas mixture of zeroed ambient air and standard gases. Standard gases such as NO, NO_2, CO, SO_2 were produced from Beijing (Beijing Hua Yuan Gas Chemical Industry Co., Ltd). O_3 standard was made from the ozone primary standard (TECO, model TE/49i). The standard gases were diluted by zero air sources with the instrument dynamic gas calibrator (TECO, 146i and 1160 Dynamic Gas Calibrator). The detailed has been described by Wang et al. (2005).

2.3 Meteorological conditions and backward trajectories

The meteorological parameters including the temperature (T), pressure (P), and relative humidity (RH) were recorded simultaneously every second with the gases

ACPD
13, 2877–2912, 2013

pollutants. The high sensitivity sensor of temperature and relative humidity (VAISALA, model: Hnp-13Y) were modified for the aircraft measurements, and the pressure sensor was made by the GLOBAL WATER Ltd. (model: WE-100).

The meteorological data from the surface areas including Beijing, Tianjin and Shijiazhuang were obtained from the website (www.wunderground.com). The gases pollutants data of the ground sites were downloaded from the local government or local environmental protection agency website (http://www.bjee.org.cn/api/index.php for Beijing, http://www.tjhb.gov.cn/ and http://221.238.254.226:95/ for Tianjin).

Back trajectories are a standard tool for determining the source regions and transport patterns of air parcels observed at receptor sites. They are good representations of the general three-dimentional wind flow and are useful in identifying particular synoptic situations (Taubman et al., 2006). All the backward trajectories were computed using the Hybrid Single-particle Lagrangian Integrated model (HYSPLIT 4) of NOAA's Air Resources Laboratory (Draxler and Rolph, 2003) with GDAS data archive.

3 Results and discussion

3.1 General description of the pollution levels at different altitudes

Three different flight routes were carried out during the sampling periods. The aircraft monitoring above Beijing city was not allowed during the Olympic periods, thus the flight routes were chosen to be carried out around Tianjin and Hebei province, the southern part of Beijing. Flight line 1 was carried out from ZJC in Tianjin to AC in Hebei, most of which is in Tianjin Province, the southeast of Beijing. Flight line 2 was carried out from AC to ZZ in Hebei, most above in the near south of Beijing. Flight line 3 was carried out among ZJC, AC, ZZ, BD, and SJZ, with two more large cities in Hebei province. Line 3 covered the region of southern part in Beijing, which could be the regional level.

For every sampling period, 48 h backward trajectories were computed at three different heights of 600 m, 900 m, 2100 m above the starting point located at ground level.

ACPD
13, 2877–2912, 2013

ZJC and AC sites for flight line 1, AC and ZZ sites for flight line 2, ZJC, AC, ZZ, BD, and SJZ sites for flight line 3 were computed. GDAS Meteorological data have been used as input (Draxler and Rolph, 2003, http://ready.arl.noaa.gov/HYSPLIT.php).

Figure 2 showed the ground level of PM_{10}, SO_2, and NO_2 in Beijing (BJ) and Tianjin (TJ) during the aircraft monitoring periods. The pollutants showed low concentrations during the period of 23–26 September, and PM_{10}, SO_2, and NO_2 were 12–31 and 22–34 $\mu g\,m^{-3}$ for PM_{10}, 6–7 and 16–24 $\mu g\,m^{-3}$ for SO_2, and 7.2–15 and 7.2–9.6 $\mu g\,m^{-3}$ for NO_2 in BJ and TJ, respectively. The higher pollution levels occurred on 28–29 August, 2 October and 13 October, and PM_{10}, SO_2, and NO_2 in BJ and TJ were 93–126 and 118–146 $\mu g\,m^{-3}$ for PM_{10}, 17–21 and 39–68 $\mu g\,m^{-3}$ for SO_2, and 11.4–84.8 and 12–18.6 $\mu g\,m^{-3}$ for NO_2, respectively, which are $3 \sim 10$ times for PM_{10}, $2 \sim 4$ times for SO_2, and $1.5 \sim 2.6$ times (except 84.8 $\mu g\,m^{-3}$ in BJ) for NO_2 of those lowest levels. Additionally, the higher level of NO_2 in BJ while SO_2 in TJ suggested the different pollution characteristics of the two cities, i.e. motor vehicles emission for BJ and coal burning emission for TJ.

Table 2 showed the average concentration of gaseous pollutants and fine particles at different heights. Consistent with the ground observations, gaseous pollutants showed correspondingly low concentrations on 25 September ($4.6 \sim 5.4$ ppbV and $0.6 \sim 0.8$ ppbV for NO_x and SO_2, respectively) below 1000 m and about 40 % decrease at 2100 m. Higher concentration was shown on higher pollutants level of ground measurements, i.e. on 27 and 28 August, 15 September, and 13 October, in accordance with the ground levels in Fig. 2.

3.2 Characteristics of gaseous pollutants at different flight routes

Based on the trajectory analysis in Figs. 3–5 and ground pollutants level in Fig. 2, the flight routes were classified into four groups with the air masses from the south, north and northwest, east, and mixed directions. The corresponding flight periods are 27 August, 28 August, 29 August, 15 September, 13 October for group 1, 1 September,

ACPD
13, 2877–2912, 2013

2 September, 11 September, 12 September, 20 September, 25 September, 27 September, 11 October for group 2, 3 and 21 September for group 3, and 8 September for group 4. The ground pollutants showed high, low and middle concentration level, respectively. The discussion will be in the order of the different groups.

3.2.1 Flights of group 1: origin of the southern transport of pollution

Group 1 flights include the 27 August and 13 October flight in line 1, 29 August flight in line 2, 28 August and 15 September flight in line 3. Most of the flights showed high concentration of gases pollutants, at all three different heights, as shown in Table 2. These flights indicated the possible influences of transport from the southern direction, and the transport influences of the polluted areas in the south part, as most from the polluted cities and industrial areas in the southern part. The gases pollutants showed some remarkable features, particularly in the air with high concentration of SO_2 and O_3, as shown in Table 2. This may be due to the stagnation with low wind speeds and highly active photochemistry, the urban emissions of both primary compounds and precursors for secondary ions lead to an additional pollutant on top of the already elevated regional level (Van Pinxteren et al., 2009; Streets et al., 2007).

As the three sites of ZJC, AC, and ZZ are in the same region, their back trajectories are similar at the same height of each flight, the middle point of the two sites ZJC and AC, AC and ZZ were used to be the representative site of the back trajectories for line 1 and 2. For line 3, three sites were used at the same time, i.e. the middle site of ZJC, AC, ZZ, BD and SJZ. Additionally, the back trajectories varied little during the same flight, and was listed only one for each flight. The detailed back trajectories for group 1 were listed in Fig. 3.

For line 1, the average SO_2 concentration of flight in group 1 (4.85 and 3.86 ppbV for 27 August and 13 October) showed tens to hundreds times higher than the average of other flights (0.03 ~ 0.69 ppbV) in 2100 m, 2 ~ 18 times higher than those other flights in 900 m (11.1 and 7.41 ppbV for 27 August and 13 October, compared with 0.62 ~ 3.37 ppbV except 17.9 ppbV on 3 September), and 2 ~ 30 times higher than those other

ACPD
13, 2877–2912, 2013

flights in 600 m (11.7 and 23.1 ppbV for 27 August and 13 October, compared with 0.78 ~ 5.19 ppbV except 22.0 ppbV on 3 September). Similar results were observed for line 2 and 3. The SO_2 concentration was 2.5 ~ 33 and 3.6 ~ 7.4 times higher than those other flights in 2100 m (6.7, 2.5, 1.2 ppbV for 29, 28 August and 15 September, compared with 0.2 ~ 2.7 ppbV for line 2 and 0.34 ppbV for line 3), 1.5 ~ 17.5 and 3.6 ~ 7.4 times higher than those other flights in 900 m (14.5 ppbV for 29 August, compared with 0.8 ~ 9.6 ppbV for line 2), 1.6 ~ 5.2 and 1.7 ~ 5.7 times higher than those other flights in 600 m (11.8, 12.9, 20.3 ppbV for 29, 28 August, and 15 September, compared with 2.3 ~ 7.2 ppbV for line 2 and 3.56 ~ 7.68 ppbV for line 3). The higher the flight, the more variation between flights of group 1 and other flights. It is obvious that the higher concentration of SO_2 especially in 2100 m may be a good tracer for the sources from regional transport.

For O_3 pollution, it showed relatively even variation at all the flights in 2100 m, as the average concentration is 40 ~ 59 ppbV, which may be the regional level of this height. However, it showed more variation between different flights at lower altitudes especially 600 m. The O_3 concentration of flights on 13 October and 15 September in group 1 showed highest concentration, and the average level is 103 and 105 ppbV, which is about 1.9 ~ 3.5 times and 1.6 ~ 1.7 times higher than those other flights in line 1 and 3. However, O_3 during other flights in group 1 on 27, 29, 28 August were not significantly high with the average level is 73, 69 and 83 ppbV, respectively. This may suggest the differences of the southern or southwestern or southeastern transport, as Fig. 3 showed. The higher O_3 concentration in 600 m on 15 September and 13 October may indicate the southwestern transport of ground pollutants, which was different from the SO_2 variation.

For NO_x pollution, all the flights showed significantly high contribution of NO_2, which contributes more than 90 % of NO_x. The NO_x was discussed only in this part. Different from the O_3 variation, the NO_x during the flights in group 1 showed higher concentration than those from other flights, and showed little different characteristics between flights of 27, 28, 29 August and 15 September and 13 October. At 2100 m, the average level

ACPD
13, 2877–2912, 2013

of NO_x on flights of 27, 28, 29 August were 17, 12, 10 ppbV, a factor of 5.3, 1.5 higher than 13 October in line 1 and 15 September in line 3. Similar results were obtained in 900 and 600 m. The higher NO_x concentration may be more from the southern or southeastern transport of ground pollutants, which showed inverse character with the O_3 pollution.

3.2.2 Flights of group 2: origin of the northwestern and northern transport of pollution

Group 2 flights include the 2, 11, 12, 25, 27 September and 11 October flight in line 1, 1 September a.m. and 20 flight in line 2, 1 September p.m. flight in line 3. Most of the flights showed generally low concentrations of gases pollutants at all three different heights, as shown in Table 2. These flights indicated the possible influences of transport from northern or northwestern direction, a clean area with low emissions of NO_x and SO_2. The detailed back trajectories were listed in Fig. 4a, b. The gases pollutants showed some remarkable features, particularly in the air with low concentration of SO_2 and O_3, as shown in Table 2.

As Fig. 2 showed, all the ground level of API pollutants in Beijing and Tianjin showed lowest concentration on 1 September and 25 September. On 1 September, the concentration of PM_{10} was 26 and 39 $\mu g\,m^{-3}$, SO_2 was 9 and 32 $\mu g\,m^{-3}$, NO_2 was 9.6 and 10.2 $\mu g\,m^{-3}$ for Beijing and Tianjin, respectively. On 25 September, the concentration of PM_{10} was 31 and 22 $\mu g\,m^{-3}$, SO_2 was 6 and 16 $\mu g\,m^{-3}$, NO_2 was 15 and 9 $\mu g\,m^{-3}$ for Beijing and Tianjin, respectively. They decreased a factor of 1.4 ~ 3.5, in comparison to the average value of other sampling periods. This may be due to the clear out of the local pollutants by the cleaner air masses from the northern or northwestern direction (Guo et al., 2004).

Correspondingly, for 600 m, the concentration of gases pollutants on 25 September was low as well, and the NO_x, SO_2, and O_3 was 5.41, 0.78, 32.2 ppbV, which was only 23 %, 8 %, and 44 % of the concentration on 27 August in line 1. While, the pollutant levels of other flights were 11.1 ~ 17.6, 1.1 ~ 5.2, 29.2 ~ 81.1 ppbV, respectively, which

ACPD
13, 2877–2912, 2013

were a factor of 2.1 ~ 3.3, 1.4 ~ 6.7, 0.9 ~ 2.5 higher than the flight on 25 September in group 2. During periods of cleaner air masses with higher wind speeds, the pollutants showed lowest concentration (Van Pinxteren et al., 2009). However, the number concentration of CN showed different characteristics on different flights, and the concentration on 25 September was 13547 N cm^{-3}, which was 1.5 times higher than those on 27 August. For other flights of group 2 in line 1, the CN concentration varies much, and the range was 7662 ~ 35725 N cm^{-3}. Similar results were obtained on the height of 900 m. While, the number concentration of CN on 2100 m was lower, and most showed a factor of 3 lower or even less than the flight on 27 August. This may indicate the characteristics of transport from the northern or northwestern direction, i.e. lower gases pollutants on all heights, lower CN on high altitudes but higher on lower altitudes. The contribution of dust in this area may be the reason.

3.2.3 Flights of group 3: origin of the eastern transport of pollution

On 8 September flight, the transport was from western direction, at 600 and 900 m, the combination of the farther sea sources and urban pollutants, as Fig. 5 shown. As the aircraft measurement was conducted on 600 and 900 m, the concentration of pollutants were compared on these two heights. For gases pollutants, it showed middle level between group 1 and group 2 in line 3, as Table 2 showed. However, the CN concentration is higher than most flights in line 3 at the two heights. This may be due to the characteristics of the sea sources, lack of gases pollutants but more sea salt particles. Additionally, the urban cities sources during the transport and local sources contribute more to the gases pollutants.

3.2.4 Flights of group 4: origin of the mixing of transport

Figure 5 showed the back trajectories of the combination between different transport directions. For 3 September flight in line 1, the transport at lower altitudes was more from the polluted southern direction but at higher altitudes more from the cleaner northern

ACPD
13, 2877–2912, 2013

direction. For 21 September, the transport at lower altitudes was more from the polluted southeastern and local sources, but at higher altitudes more from the farther northwestern direction. Similarly to other observations (Van Pinxteren et al., 2009), the lengths of the back trajectories are much shorter for the south direction flights at lower altitudes, and slow movement of air masses in the south direction favors the accumulation of pollution before arriving at the sampling sites. While, the lengths of the back trajectories for the north or northwest direction are much longer at higher altitudes, and the quick movement of the air masses favors the clean effects on pollutants.

These flights showed the influences of the different transport directions for the pollutants. The combination between different transport directions made the pollutants level in the middle of the group 1 and group 2.

The gases concentration on 3 September flight showed clear vertical gradient. The NO_x showed the lowest concentration at 2100 m (4.0 ppbV), and increased by a factor of 3.2 and 3.8 on 900 and 600 m (13.7 and 16.5 ppbV), respectively. While, the SO_2 on 2100 m was only 0.13 ppbV, but significantly enhanced at 900 and 600 m by a factor of 138 and 169, respectively. This may again verify that SO_2 was a good tracer for polluted southern transport or local pollutants, compared with the NO_x. The O_3 concentration was 47 ppbV at 2100 m, which is a little higher than those group 2 (40 ~ 45.5 ppbV) and lower than group 1 (55 ~ 59 ppbV), but showed 88.3 and 95.7 ppbV on 900 and 600 m, which was 20 ~ 32 %, −6.86 ~ 31 % higher than those group 1 (67.0 ~ 74.7 ppbV and 73.3 ~ 102.7 ppbV for 900 and 600 m) and 1.8 ~ 2.7, 1.7 ~ 3.0 times higher than those group 2 (32.9 ~ 48.7 ppbV and 32.2 ~ 55.2 ppbV for 900 and 600 m). This may again verify that the O_3 could be a possible tracer for the southern direction transport and local pollutants. However, the O_3 was not so good as SO_2, as the high value of regional level, just as group 2 showed.

3.3 Variation of the long-lived gas CO

Different from the reactive gases of NO_x, SO_2, and O_3, CO was long lived and non-active. It can be transported for a long range, and could be used as a potential tracer of

ACPD
13, 2877–2912, 2013

long range transport. However, local sources of CO are complicated, and may be mixed with transport sources. The variation of different heights showed different characteristics even in the same groups. Figure 6 showed the variation of CO concentration at different heights during different flights, only a few flights were listed as examples here.

As pollutants of the higher altitudes transport longer or different from the lower altitudes, the CO variation was discussed between different heights. For line 1, three different classes of flights were obtained, i.e. lower at 2100 m but higher at lower altitudes, higher at 2100 m but lower at lower altitudes, similar on all altitudes. The first class of flights included the flight on 27 August and 3 September. It showed lowest CO level on the highest altitudes, and increased with the decrease of the altitudes. The concentration at 2100 m was 0.12 ppmV for 27 August, and below the detection limit for 3 September, but increased to 0.48, 0.35 ppmV at 900 m and 0.61, 0.32 ppmV at 600 m, respectively. Back trajectory analysis for the flights showed the differences, i.e. the longer transport of higher altitudes at 2100 m (northwestern direction on 27 August and northern on 3 September) and shorter or regional sources on lower altitudes (southern direction and regional sources on 27 August and 3 September). The second class of flights included the flight on 2 September, 11 September, and 25 September. It showed the highest CO level at the highest altitudes, and decreased with the increase of the altitudes. The concentration at 2100 m was 0.33, 0.53, and 0.70 ppmV on 2 September, 11 September, and 25 September, respectively, but decreased about 30 ~ 45 % at 900 m and 46 ~ 67 % at 600 m. Different from the class 1 flights, the back trajectories showed the same northwestern transport direction at the three heights but transport longer at 2100 m, as Fig. 4a showed. The northwestern direction at lower altitudes had a "cleaner" effect on the local and regional CO pollution, which has been reported on the influences of the dust storm (Guo et al., 2004). The high concentration of 2100 m may show the transport effect from northwestern direction on higher altitude. This showed that CO may be a good tracer for northwestern direction on 2100 m when all the heights showed the same transport direction, with the consideration of the class 1 flights. The third class of flights included the flight in the morning and afternoon

ACPD
13, 2877–2912, 2013

on 11 October and 13 October. It showed similar level at the three heights of the same flight, and the CO level was 0.37 ~ 0.52, 0.14 ~ 0.18, and 0.53 ~ 1.15 ppmV, respectively. The back trajectories showed the combination of class 1 and class 2 above. However, it is different for flights on 11 October and 13 October, i.e. the same transport direction and similar transport range at the three heights on 11 October, but the longer transport western direction on 2100 m and southwestern direction on 900 m and 600 m. The "cleaner" effect from the northwestern transport direction made the CO level on the afternoon flight significantly lower than the morning flight, as Fig. 6 and Table 2 showed.

3.4 Size distribution of particles and its influencing factors

Different from those gases pollutants, the number concentration of particles (CN and $PM_{0.5}$) showed not much relationship with ground sources, as shown in Table 2. While, similar to the gaseous pollutants, the concentrations of particles were always high when the air masses were from the southern, consistent with previous observations (Van Pinxteren et al., 2009; Guinot et al., 2007; Wang et al., 2005; Wehner et al., 2008). Van Pinxteren et al. (2009) has investigated two factors which are discussed below. Firstly, the surrounding areas of Beijing show different characteristics, for example, the south direction are highly populated and industrialized, while the north or northwest direction and partially eastern regions are mountains or deserts with less anthropogenic influences. Thus air masses from the southern areas are influenced by high pollution emissions and those from northern areas are influenced by less anthropogenic emissions. Secondary, wind speeds have been reported to be often lower during southern advection (Wehner et al., 2008), as was the case during this study. Similar to other observations (Van Pinxteren et al., 2009), the lengths of the back trajectories are much shorter for the south direction flights (see Figs. 3–5), and slow movement of air masses in the south direction favors the accumulation of pollution before arriving to the sampling sites.

ACPD
13, 2877–2912, 2013

However, the size distribution of particles showed different characteristics at different heights and different transport direction. The flight route of 27 August was discussed in detail in the following.

Figure 7 showed the variation of size distributions with the altitudes. Obviously, the size distribution at 2100 m was different from those on lower altitudes, and the peaks concentrated on smaller sizes of 20 ~ 30 nm. While, for the lower altitudes, the peaks concentrated on larger sizes of 80 ~ 120 nm. Additionally, the size distribution showed different characteristics at different flight areas, and the peaks shifted to smaller sizes at special flight areas, as shown in Fig. 7.

Sources emission and regional transport may be the major factors affecting the size distribution of particles. Sources from different transport directions showed different characteristics at different heights, i.e. northwestern direction at 2100 m and southern direction at 900 m and 600 m on 27 August flight, as shown in Fig. 3. Correspondingly, the size distribution of 5.6–560 nm particles showed peaks of 20 ~ 30 nm at 2100 m and 80 ~ 120 nm at 900 m and 600 m. While, it showed no peaks at 2100 m and showed peaks of ~ 0.7 μm at 900 m and 600 m at size range of 0.5 ~ 20 μm, as shown in Fig. 8. This may indicate the influencing effects of the different transport directions, i.e. the cleaner effects of northwestern and polluted effects of southern transportation, which may be consistent with other ground-based researches (Van Pinxteren et al., 2009; Guinot et al., 2007; Wang et al., 2005; Wehner et al., 2008).

Additionally, ground sources affect the particles below 1000 m most and no obvious influences on those at 2100 m. As it is shown in Fig. 7, the size distribution of particles 5.6–560 nm varied much at different flight areas at 900 m and 600 m, and the peaks of size distribution showed tendency to smaller sizes at 4:05 ~ 4:08, 4:12 ~ 4:16, and 4:43 ~ 4:49 a.m. (GMT) at 900 m. Similar results are shown for size distribution at 600 m. The detailed size distribution is shown in Fig. 8, and the average size distribution of the three different time ranges above on 900 m was also indicated as an example. Obviously, the size distributions peak at 81 nm at 900 m for the average of special flight areas, and 93 nm on other average flight areas at both 600 m and

ACPD
13, 2877–2912, 2013

900 m. As the aircraft measurements were conducted in linear flight between two sites, the detailed longitude and latitude were got, and it was in the range of 39°17.81′ N, 117°24.43′ E ~ 39°21.01′ N, 117°13.32′ E. During the longitude and latitude ranges of ground sources, several highways and freeways were connected in these areas, i.e. Jingjin highways, Jinyu freeways connected with local roads. Figure 9 showed the average size distribution of particles at different heights on 27 August flight, and the peak above the highway was specially noted.

However, we didn't observe similar 81 nm peaks during other flights even at the same flight areas. The meteorological information may contribute this. There was a moderate rain to thunderstorm on 27 August (www.wunderground.com). The wet deposition helps scavenge the aged particles (Nilsson, et al., 2001; Elperin et al., 2011). Freshly emission from vehicles was observed, which was consistent with results from Wang et al. (2011). They conducted the on-road emissions of individual diesel vehicles in and around Beijing by a mobile platform equipped with fast response instruments such as EEPS, and got bimodal modes peaking around 10 nm and 80 nm, similar to 81 nm in special flight areas in this study. This confirms the potential impacts from vehicles emission of highways or freeways, in addition to the meteorological factors.

4 Summary and conclusion

Intensive aircraft measurements of gaseous pollutants and particles in the Beijing surrounding areas were conducted during 27 August to 13 October. It was made during typical flights at altitudes of 600, 900, and 2100 m along three different flight routes. Major findings include:

1. Based on the back trajectories and pollution variation, the flights were classified into four groups, i.e. polluted air from the southern transport direction, cleaner air from the northern or northwestern transport direction, the mixing from the north and south transport direction, and eastern transport direction.

ACPD
13, 2877–2912, 2013

2. Flights of group 1: origin of the southern transport of pollution. The higher concentration of SO_2 especially at 2100 m may be a good tracer for the sources from southern transport. The higher NO_x concentration may be more from the southern or southeastern transport of ground pollutants, which showed inverse character with the O_3 pollution.

3. Flights of group 2: origin of the northwestern and northern transport of pollution. Most of the flights showed lowest concentration of gases pollutants, at all three different heights. These flights indicated the possible influences of transport from the cleaner northern or northwestern direction, and the characteristics of transport was lower gases pollutants on all heights, lower CN on high altitudes but higher on lower altitudes. The contribution of deserted areas in this area may be the reason.

4. Flights of group 3: origin of the eastern transport of pollution. For gases pollutants, it showed middle level between group 1 and group 2. However, the CN concentration is higher than most flights at the two heights. This may be due to the characteristics of the sea sources, lack of gases pollutants but more sea salt particles. Additionally, the urban cities sources during the transport and local sources contribute more to the gases pollutants.

5. Flights of group 4: origin of the mixing of transport. It means that the transport at lower altitudes was more from the polluted southern direction, but at higher altitudes more from the cleaner northern direction. Additionally, the lengths of the back trajectories are much shorter for the south direction flights at lower altitudes, and slow movement of air masses in the south direction favors the accumulation of pollution before arriving to the sampling sites. While, the lengths of the back trajectories for the north or northwest direction are much longer at higher altitudes, and the quick movement of the air masses favors the clean effects from the deserted or less anthropogenic transport influences. These flights showed the influences of the different transport for the pollutants. The combination between different transport made the pollutants level in the middle of the group 1 and group

ACPD
13, 2877–2912, 2013

2. It may verify that the O_3 could be a possible tracer for the southern direction transport and local pollutants, although not so representative as SO_2.

6. Different from the reactive gases of NO_x, SO_2, and O_3, CO was long lived and non-active. It can be transported for a long range, and could be used as a possible tracer of long range transport. However, local sources of CO are complicated, and may be mixed with transport sources. The variation of different heights showed different characteristics even at the same groups. Results showed that CO may be a good tracer for northwestern direction on 2100 m when all the heights showed the same transport direction, with the consideration of the class 1 flights.

7. The variation of size distribution of 5.6 ~ 560 nm particles showed three influencing factors, i.e. transport direction, ground emission sources and meteorological factors. Take the flight 27 August as an example, the different transport direction contribute the different size distribution at 2100 m and lower altitudes. For northwestern transport of 2100 m, the peaks concentrated on 20 ~ 30 nm. While, for the southern transport of lower altitudes, the peaks concentrated on larger sizes of 80 ~ 120 nm. Additionally, the peaks shifted to smaller sizes above the special highways or freeways influenced areas. The ground sources influence much to the particles below 1000 m and no obvious influences on 2100 m. While, the wet deposition on 27 August helps scavenge the aged particles and the emission of freshly emission from vehicles, which could explain the phenomenon was not observed on other flights.

Acknowledgements. This work was supported by the CAREBeijing-2008 project, the NSFC project (41205115), and the special fund of State Key Joint Laboratory of Environment Simulation and Pollution Control (11K02ESPCP). The authors gratefully acknowledge the NOAA Air Resources laboratory (ARL) for the provision of the HYSPLIT transport and dispersion model and READY website used in this paper.

ACPD
13, 2877–2912, 2013

References

Beijing Organizing Committee for the Games of the XXIX Olympic Games (BOCOG): Green Olympics in Beijing 2005, available at: http://en.beijing2008.cn/30/79/article212027930.shtml, 2005.

Dickerson, R. R., Li, C., Li, Z., Marufu, L. T., Stehr, J. W., McClure, B., Krotkov, N., Chen, H., Wang, P., Xia, X., Ban, X., Gong, F., Yuan, J., and Yang, J.: Aircraft observations of dust and pollutants over northeast China: insight into the meteorological mechanisms of transport, J. Geophys. Res., 112, D24S90, doi:10.1029/2007JD008999, 2007.

Draxler, R. R. and Rolph, G. D.: HYSPLIT (HYbrid Single-Particle Lagrangian Integrated Trajectory) Model access via NOAA ARL READY Website NOAA Air Resources Laboratory, Silver Spring, MD, available at: http://ready.arl.noaa.gov/HYSPLIT.php, 2003.

Elperin, T., Fominykh, A., Krasovitov, B., and Vikhansky, A.: Effect of rain scavenging on altitudinal distribution of soluble gaseous pollutants in the atmosphere, Atmos. Environ., 45, 2427–2433, 2011.

Garland, R. M., Schmid, O., Nowak, A., Achtert, P., Wiedensohler, A., Gunthe, S. S., Takegawa, N., Kita, K., Kondo, Y., Hu, M., Shao, M., Zeng, L. M., Zhu, T., Andreae, M. O., and Pöschl, U.: Aerosol optical properties observed during Campaign of air quality research in Beijing 2006 (CAREBeijing-2006): characteristic differences between the inflow and outflow of Beijing city air, J. Geophys. Res., 114, D00G04, doi:10.1029/2008JD010780, 2009.

Guinot, B., Cachier, H., Sciare, J., Tong, Y., Xin, W., and Jianhua, Y.: Beijing aerosol: atmospheric interactions and new trends, J. Geophys. Res., 112, D14314, doi:10.1029/2006JD008195, 2007.

Guo, J., Rahn, K. A., and Zhuang, G.: A mechanism for the increase of pollution elements in dust storms in Beijing, Atmos. Environ., 38, 855–862, 2004.

Heland, J., Ziereis, H., Schlager, H., de Reus, M., Traub, M., Lelieveld, J., Roelofs, G.-J., Stock, P., and Roiger, A.: Aircraft measurements of nitrogen oxides, ozone, and carbon monoxide during MINOS 2001: distributions and correlation analyses, Atmos. Chem. Phys. Discuss., 3, 1991–2026, doi:10.5194/acpd-3-1991-2003, 2003.

Huang, X.-F., He, L.-Y., Hu, M., Canagaratna, M. R., Sun, Y., Zhang, Q., Zhu, T., Xue, L., Zeng, L.-W., Liu, X.-G., Zhang, Y.-H., Jayne, J. T., Ng, N. L., and Worsnop, D. R.: Highly time-resolved chemical characterization of atmospheric submicron particles during 2008 Beijing

ACPD
13, 2877–2912, 2013

Olympic Games using an Aerodyne High-Resolution Aerosol Mass Spectrometer, Atmos. Chem. Phys., 10, 8933–8945, doi:10.5194/acp-10-8933-2010, 2010.
Huebert, B., Bertram, T., Kline, J., Howell, S., Eatough, D., and Blomquist, B.: Measurements of organic and elemental carbon in Asian outflow during ACE-Asia from the NSF/NCAR C-130, J. Geophys. Res., 109, D19S11, doi:10.1029/2004JD004700, 2004.
Jung, J., Lee, H., Kim, Y. J., Liu, X., Zhang, Y., Hu, M., and Sugimoto, N.: Optical properties of atmospheric aerosols obtained by in situ and remote measurements during 2006 Campaign of air quality research in Beijing (CAREBeijing-2006), J. Geophys. Res., 114, D00G02, doi:10.1029/2008JD010337, 2009.
Kawamura, K., Umemoto, N., Mochida, M., Bertram, T., Howell, S., and Huebert, B. J.: Water-soluble dicarboxylic acids in the tropospheric aerosols collected over east Asia and western North Pacific by ACE-Asia C-130 aircraft, J. Geophys. Res., 108, 8639, doi:10.1029/2002JD003256, 2003.
Li, Z., Chen, H., Cribb, M., Dickerson, R., Holben, B., Li, C., Lu, D., Luo, Y., Maring, H., Shi, G., Tsay, S.-C., Wang, P., Wang, Y., Xia, X., Zheng, Y., Yuan, T., and Zhao, F.: Preface to special section on East Asian Studies of Tropospheric Aerosols: an international regional experiment (EAST-AIRE), J. Geophys. Res., 112, D22S00, doi:10.1029/2007JD008853, 2007.
Matsui, H., Koike, M., Kondo, Y., Takegawa, N., Kita, K., Miyazaki, Y., Hu, M., Chang, S.-Y., Blake, D. R., Fast, J. D., Zaveri, R. A., Streets, D. G., Zhang, Q., and Zhu, T.: Spatial and temporal variations of aerosols around Beijing in summer 2006: model evaluation and source apportionment, J. Geophys. Res., 114, D00G13, doi:10.1029/2008JD010906, 2009.
Nilsson, E. D., Paatero, J. and Boy, M.: Effects of air masses and synoptic weather on aerosol formation in the continental boundary layer, Tellus B, 53, 462–478, 2001.
Simoneit, B. R. T., Kobayashi, M., Mochida, M., Kawamura, K., and Huebert, B. J.: Aerosol particles collected on aircraft flights over the northwestern Pacific region during the ACE-Asia campaign: compositions and major sources of the organic compounds, J. Geophys. Res., 109, D19S10, doi:10.1029/2004JD004565, 2004.
Streets, D. G., Fu, J. S., Jang, C. J., Hao, J., He, K., Tang, X., Zhang, Y., Wang, Z., Li, Z., Zhang, Q., Wang, L., Wang, B., and Yu, C.: Air quality during the 2008 Beijing Olympic Games, Atmos. Environ., 41, 480–492, 2007.
Takegawa, N., Miyakawa, T., Kuwata, M., Kondo, Y., Zhao, Y., Han, S., Kita, K., Miyazaki, Y., Deng, Z., Xiao, R., Hu, M., van Pinxteren, D., Herrmann, H., Hofzumahaus, A., Holland, F., Wahner, A., Blake, D. R., Sugimoto, N., and Zhu, T.: Variability of submicron aerosol ob-

ACPD
13, 2877–2912, 2013

served at a rural site in Beijing in the summer of 2006, J. Geophys. Res., 114, D00G05, doi:10.1029/2008JD010857, 2009.
Taubman, B. F., Hains, J. C., Thompson, A. M., Marufu, L. T., Doddridge, B. G., Stehr, J. W., Piety, C. A., and Dickerson, R. R.: Aircraft vertical profiles of trace gas and aerosol pollution over the mid-Atlantic U.S.: statistics and meteorological cluster analysis. J. Geophys. Res., 111, D10S07, doi:10.1029/2005JD006196, 2006.
TSI: The features and benefits of the Engine Exhaust Particle Sizer spectrometer model 3090, available at: http://www.tsi.com/Engine-Exhaust-Particle-Sizer-Spectrometer-3090/, 2013.
Tu, F. H., Thornton, D. C., Bandy, A. R., Kim, M., Carmichael, G., Tang, Y., Thornhill, L., and Sachse, G.: Dynamics and transport of sulfur dioxide over the Yellow Sea during TRACE-P, J. Geophys. Res., 108, 8790, doi:10.1029/2002JD003227, 2003.
Van Pinxteren, D., Brüggemann, E., Gnauk, T., Iinuma, Y., Müller, K., Nowak, A., Achtert, P., Wiedensohler, A., and Herrmann, H.: Size- and time-resolved chemical particle characterization during CAREBeijing-2006: different pollution regimes and diurnal profiles, J. Geophys. Res., 114, D00G09, doi:10.1029/2008JD010890, 2009.
Wang, G., Kawamura, K., Hatakeyama S., Takami, A., Li, H., and Wang, W.: Aircraft measurement of organic aerosols over China, Environ. Sci. Technol., 41, 3115–3120, 2007.
Wang, W., Liu, H., Yue, X., Li, H., Chen, J., and Tang, D.: Study on size distribution of airborne particles by aircraft observation in spring over eastern coastal areas of China, Adv. Atmos. Sci., 22, 328–336, 2005.
Wang, W., Bao, L. F., Liu, H. J., Yue, X., Chen, J. H., Li, H., Ren, L. H., Tang, D. G., Hatakeyama, S., and Takami, A.: Vertical profiles of aerodynamic size distribution for airborne particles over Yangtze River Delta, Chinese Phys., 16, 2818–2824, 2007.
Wang, W., Ma, J., Hatakeyama, S., Liu, X., Chen, Y., Takami, A., Ren, L., and Geng, C.: Aircraft measurements of vertical ultrafine particles profiles over Northern China coastal areas during dust storms in 2006, Atmos. Environ., 42, 5715–5720, 2008a.
Wang, W., Ren, L., Zhang, Y., Chen, J., Liu, H., Bao, L., Fan, S., and Tang, D.: Aircraft measurements of gaseous pollutants and particulate matter over Pearl River Delta in China, Atmos. Environ., 42, 6187–6202, 2008b.
Wang, X., Westerdahl, D., Wu, Y., Pan, X., and Zhang, K. M.: On-road emission factor distributions of individual diesel vehicles in and around Beijing, China, Atmos. Environ., 45, 503–513, 2011.

ACPD
13, 2877–2912, 2013

Wang, Y., Zhuang, G. S., Tang, A. H., Yuan, H., Sun, Y. L., Chen, S., and Zheng, A. H.:: The ion chemistry and the source of $PM_{2.5}$ aerosol in Beijing, Atmos. Environ., 39, 3771–3784, doi:10.1016/j.atmosenv.2005.03.013, 2005.

Wehner, B., Birmili, W., Ditas, F., Wu, Z., Hu, M., Liu, X., Mao, J., Sugimoto, N., and Wiedensohler, A.: Relationships between submicrometer particulate air pollution and air mass history in Beijing, China, 2004–2006, Atmos. Chem. Phys., 8, 6155–6168, doi:10.5194/acp-8-6155-2008, 2008.

Yue, D., Hu, M., Wu, Z., Wang, Z., Guo, S., Wehner, B., Nowak, A., Achtert, P., Wiedensohler, A., Jung, J., Kim, Y. J., and Liu, S.: Characteristics of aerosol size distributions and new particle formation in the summer in Beijing, J. Geophys. Res., 114, D00G12, doi:10.1029/2008JD010894, 2009.

Zhang, Q., Zhao C., Tie, X., Wei, X., Huang, M., Li, G., Ying, Z., and Li, C.: Characterizations of aerosols over the Beijing region: a case study of aircraft measurements, Atmos. Environ., 40, 4513–4527, 2006.

Zhang, Q., Ma, X., Tie, X., Huang, M., and Zhao C.: Vertical distributions of aerosols under different weather conditions: Analysis of in-situ aircraft measurements in Beijing, China, Atmos. Environ., 43, 5526–5535, 2009.

ACPD
13, 2877–2912, 2013

Table 1. The flight time, range, pattern, area and related information for different flight line.

Line	Date	Time	Altitude Range	Pattern	Flight Area
1	27 Aug 2008	10:35 ~ 14:25	2100 ~ 900 ~ 600	Linear, back and forth	ZJ(39°17′, 117°27′ E) ~ AC(39°31′ N, 116°42′ E)
	2 Sep 2008	14:13 ~ 17:53	2100 ~ 900 ~ 600		
	3 Sep 2008	9:41 ~ 13:33	2100 ~ 900 ~ 600		
	11 Sep 2008	9:09 ~ 13:04	2100 ~ 900 ~ 600		
	12 Sep 2008	8:50 ~ 12:43	2100 ~ 900 ~ 600		
	25 Sep 2008	14:00 ~ 18:04	2100 ~ 900 ~ 600		
	27 Sep 2008	9:07 ~ 12:16	900 ~ 600		
	11 Oct 2008	9:15 ~ 13:20	2100 ~ 900 ~ 600		
		13:46 ~ 17:40	2100 ~ 900 ~ 600		
	13 Oct 2008	12:50 ~ 16:42	2100 ~ 900 ~ 600		
2	29 Aug 2008	9:04 ~ 12:54	2100 ~ 900 ~ 600	Linear, back and forth	AC(39°31′ N, 116°42′ E) ~ ZZ(39°29′ N, 115°58′ E)
	1 Sep 2008	8:44 ~ 12:37	2100 ~ 900 ~ 600		
	20 Sep 2008	10:06 ~ 13:20	2100 ~ 900		
	21 Sep 2008	9:09 ~ 14 : 30	2100 ~ 900 ~ 600		
3	28 Aug 2008	8:57 ~ 13:06	2100 ~ 600	Linear, back and forth	ZJ ~ AC ~ ZZ~ BD(38°52′ N, 115°28′ E) ~ SJ(38°3′ N, 114°31′ E)
	1 Sep 2008	15:04 ~ 18:25	2100 ~ 600		
	8 Sep 2008	13:55 ~ 17:27	900 ~ 600		
	15 Sep 2008	13:25 ~ 17:18	2100 ~ 600		
Line 1 Total		10 flights, 2283 min (38 h), 3 heights			
Line 2 Total		4 flights, 970 min (16.2 h), 3 heights			
Line 3 Total		4 flights, 887 min (14.8 h), 3 heights			

ACPD
13, 2877–2912, 2013

Table 2. The average concentration of gases pollutants and condensable nuclei concentrations at different heights of each flight (the unit of CN, $PM_{0.5}$ are N cm^{-3}, CO is ppmV, and other gases are ppbV).

Height	Line	1						2							3				
	Date	8–27^{a}	9–2^{p}	9–3^{a}	9–11^{a}	9–12^{a}	9–25^{p}	9–27^{a}	10–11^{a}	10–11^{p}	10–13^{p}	8–29^{a}	9–1^{a}	9–20^{a}	9–21^{ap}	8–28^{a}	9–1^{p}	9–8^{p}	9–15^{p}
2100	NO_2	16.36	4.42	3.88	8.37	6.44	2.20	–	1.20	2.54	2.43	9.42	8.93	4.63	4.60	11.36	6.09	–	7.68
	NO	0.52	0.37	0.44	0.39	0.41	0.39	–	0.35	0.44	0.76	0.35	0.35	0.47	0.43	0.42	0.39	–	0.44
	NO_x	16.88	4.79	4.31	8.76	6.84	2.59	–	1.55	2.98	3.20	9.77	9.28	5.10	4.88	11.78	6.48	–	8.12
	SO_2	4.85	0.38	0.13	0.34	0.33	0.42	–	0.69	0.03	3.86	6.73	0.21	2.72	1.05	2.50	0.34	–	1.22
	O_3	58.64	51.82	47.15	42.15	44.14	39.66	–	43.39	45.47	55.25	66.85	46.60	59.00	51.63	58.87	49.36	–	53.65
	CO	0.12	0.33	–	0.53	0.24	0.70	–	0.52	0.15	0.83	0.05	–	0.46	0.33	0.13	–	–	0.35
	CN	3144	8518	–	1381	–	1112	–	–	–	3900	–	629	3763	734	–	8507	–	8496
	$PM_{0.5}$	14691	5073	–	2527	1999	2877	–	1435	1849	5771	4141	2692	6574	3481	3621	5381	–	5561
900	NO_2	18.54	9.62	12.42	16.18	13.01	4.04	3.12	0.63	5.86	6.62	10.81	8.47	6.67	13.07	11.48	–	11.08	–
	NO	1.49	0.46	1.28	0.48	0.65	0.54	0.45	1.95	1.23	0.50	0.56	0.47	0.47	0.84	0.45	–	0.58	–
	NO_x	20.03	10.08	13.70	16.66	13.66	4.58	3.56	2.58	7.10	7.12	11.37	8.73	7.14	13.91	11.93	–	11.65	–
	SO_2	11.10	3.37	17.93	1.19	1.33	0.65	0.54	0.62	0.99	7.41	14.54	0.83	4.82	9.62	7.64	–	8.62	–
	O_3	67.03	69.31	88.26	48.69	46.69	32.89	34.76	35.61	39.44	74.73	73.59	44.88	67.77	69.77	63.69	–	74.80	–
	CO	0.48	0.18	0.35	0.30	0.26	0.49	0.43	0.37	0.14	0.53	0.09	–	0.65	0.56	0.06	–	0.76	–
	CN	8288	16353	11508	14880	8916	20770	964	8918	5941	9193	–	2778	1805	9384	–	–	15141	–
	$PM_{0.5}$	12123	16114	–	12963	8695	23321	6267	9654	10671	12080	10663	11277	4936	–	7100	–	18609	–
600	NO_2	22.15	14.17	15.61	17.06	16.91	5.02	8.68	9.31	10.35	17.49	20.56	14.30	–	7.83	17.33	12.17	16.06	18.92
	NO	1.13	0.45	0.90	0.51	0.49	0.39	3.27	3.68	0.74	0.63	0.78	1.58	–	0.48	0.74	0.56	0.80	0.82
	NO_x	23.28	14.62	16.51	17.58	17.40	5.41	11.96	12.99	11.09	18.12	21.34	15.88	–	8.31	18.07	12.73	16.86	19.74
	SO_2	11.68	5.19	21.99	2.49	1.05	0.78	13.60	2.14	1.75	23.11	11.83	2.29	–	7.18	12.88	3.56	7.68	20.30
	O_3	73.25	81.13	95.65	55.16	48.91	32.19	29.21	34.81	41.72	102.69	82.77	49.98	–	66.97	68.80	60.59	67.48	104.68
	CO	0.61	0.11	0.32	0.21	0.15	0.38	0.89	0.42	0.18	1.15	0.19	–	–	0.63	0.62	–	0.90	1.00
	CN	8829	13034	12280	25835	7662	13547	16439	35725	10954	17016	–	6936	–	5402	–	6453	15508	20945
	$PM_{0.5}$	14653	20147	–	15924	10183	17127	70722	29343	12925	19824	14356	17764	–	10883	12805	13642	17466	30670

The superscript a and p means the a.m. and p.m. of that sampling day, – means no detection or below the limit.

ACPD
13, 2877–2912, 2013

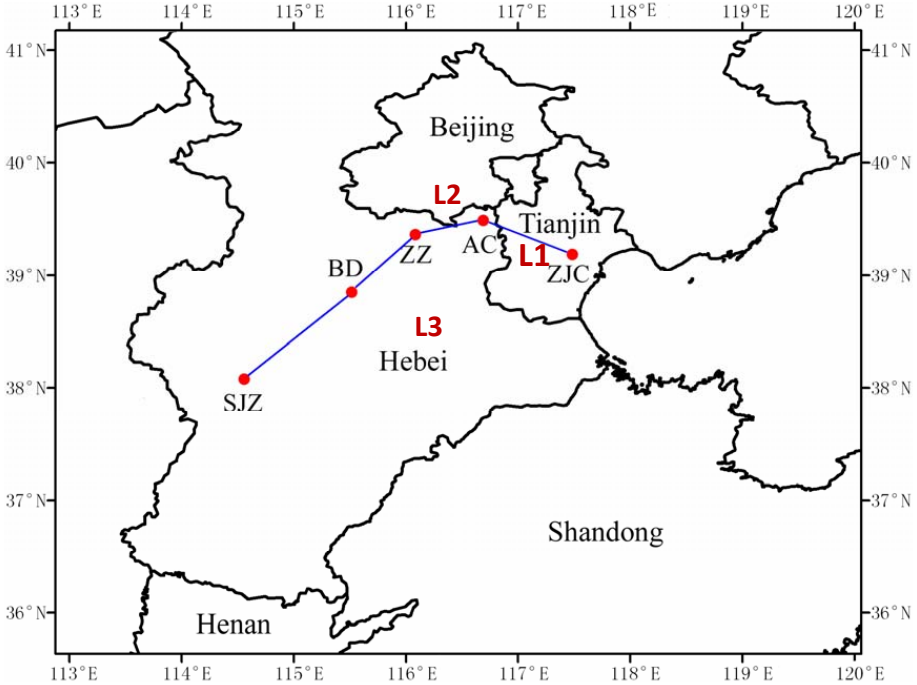

Fig. 1. The three flight routes during the aircraft sampling periods (ZJC, AC, ZZ, BD, and SJZ means the start and end sampling sites Zaojiacheng, Anci, Zhuozhou, Baoding, and Shijiazhuang).

ACPD
13, 2877–2912, 2013

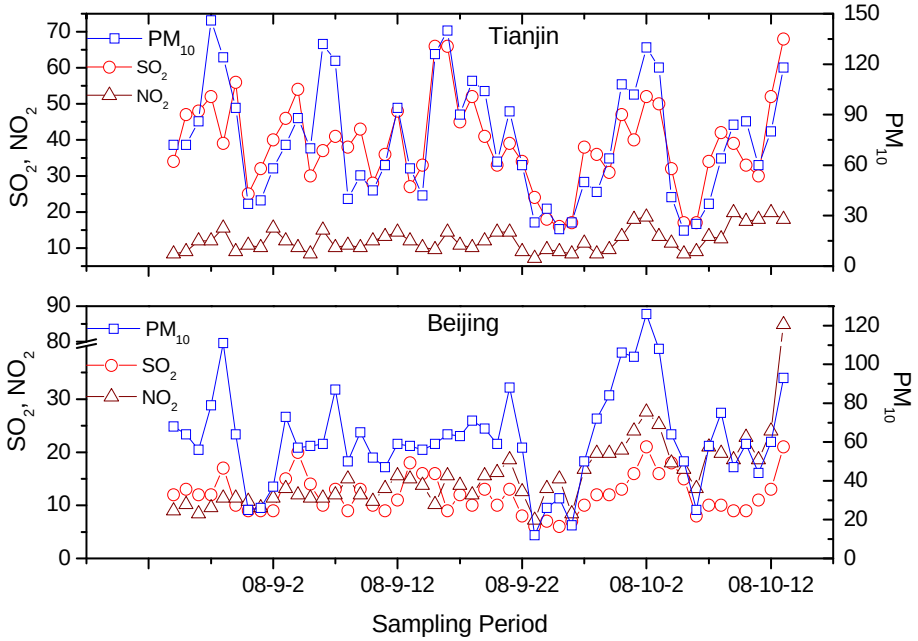

Fig. 2. The ground level of API pollutants during sampling periods ($\mu g\,m^{-3}$).

ACPD
13, 2877–2912, 2013

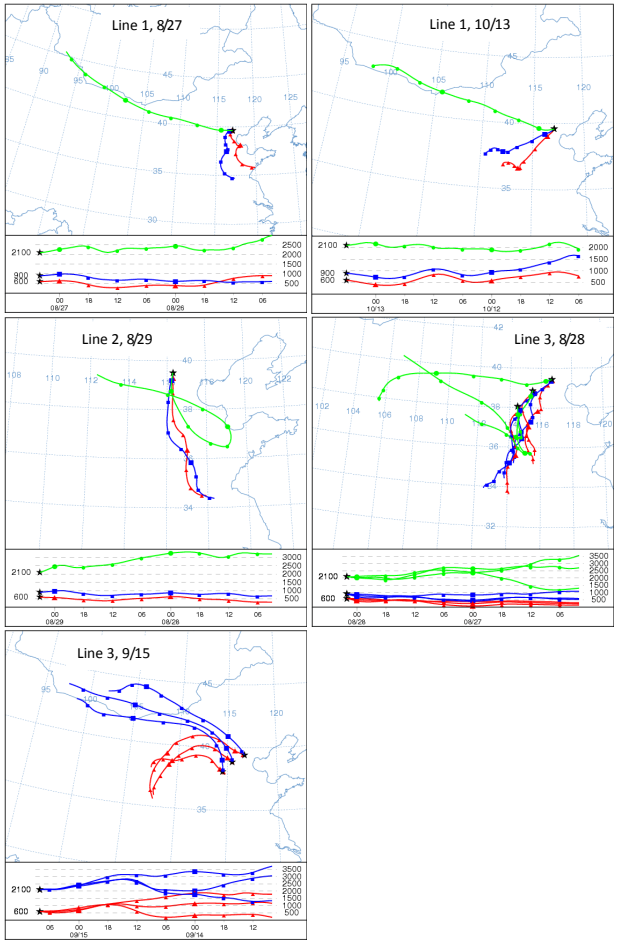

Fig. 3. A 48 h back trajectories for line 1 (39.6° N, 117.075° E), line 2 (39.5° N, 116.3° E) and line 3 (39.43° N, 116.7° E; 38.87° N, 115.47° E; 38.05° N, 114.5° E) of the group 1 flights.

ACPD
13, 2877–2912, 2013

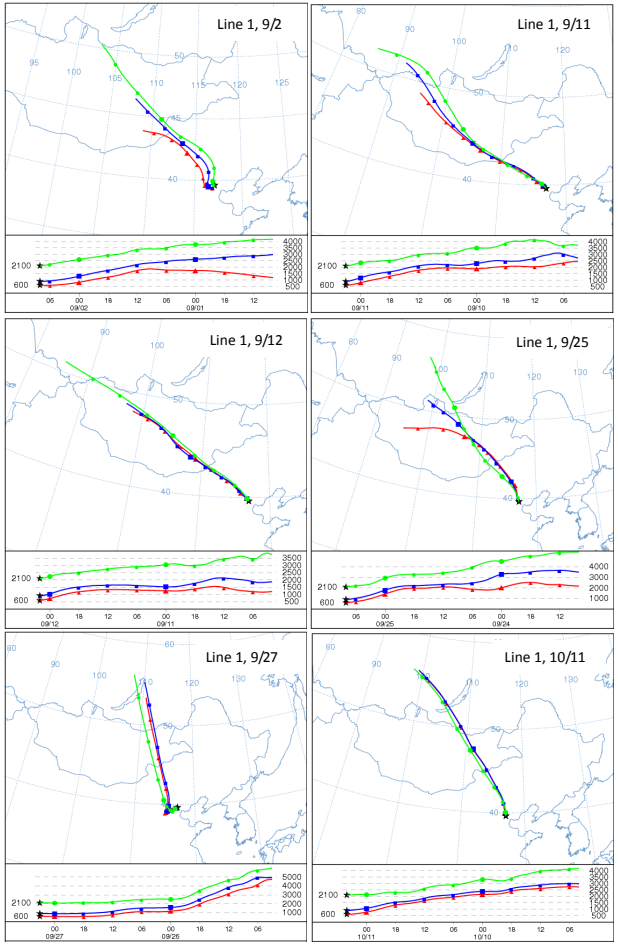

Fig. 4a. A 48 h back trajectories of the group 2 flights for line 1 (39.6° N, 117.075° E).

ACPD
13, 2877–2912, 2013

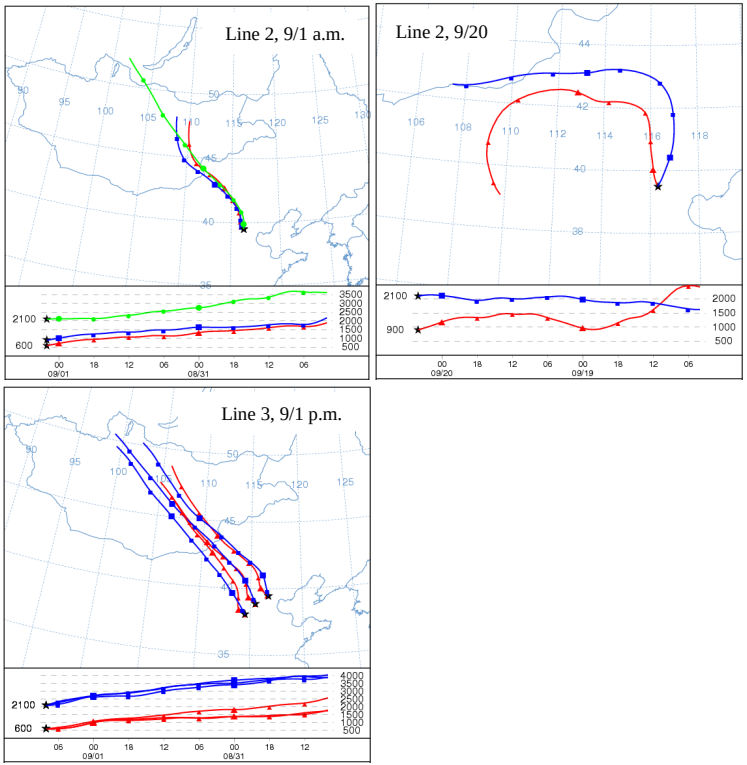

Fig. 4b. A 48 h back trajectories of the group 2 flights for line 2 (39.5° N, 116.3° E) and line 3 (39.43° N, 116.7° E; 38.87° N, 115.47° E; 38.05° N, 114.5° E).

ACPD
13, 2877–2912, 2013

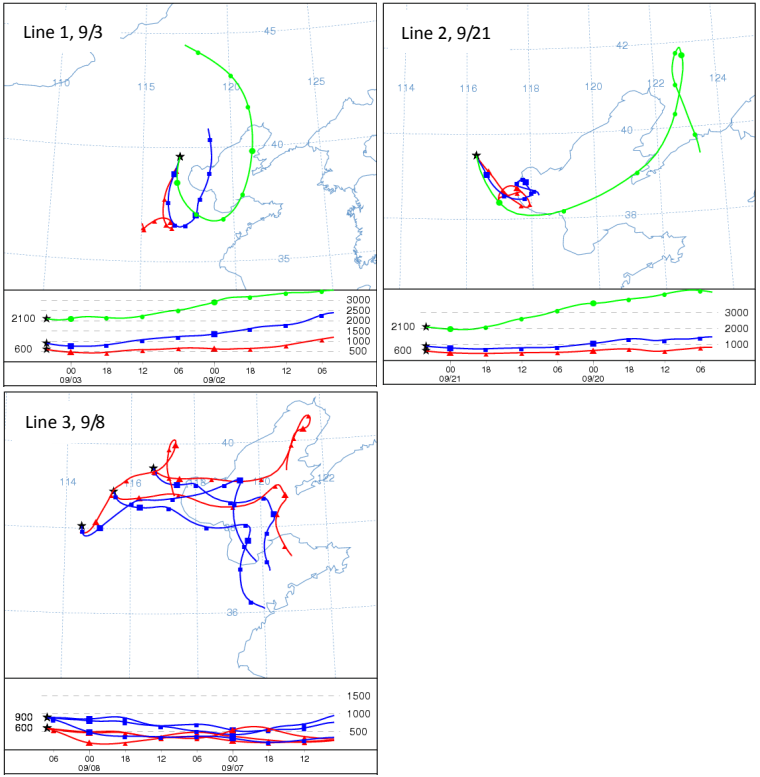

Fig. 5. A 48 h back trajectories for line 1 (39.6° N, 117.075° E), line 2 (39.5° N, 116.3° E) and line 3 (39.43° N, 116.7° E; 38.87° N, 115.47° E; 38.05° N, 114.5° E) of the group 3 and 4 flights.

ACPD
13, 2877–2912, 2013

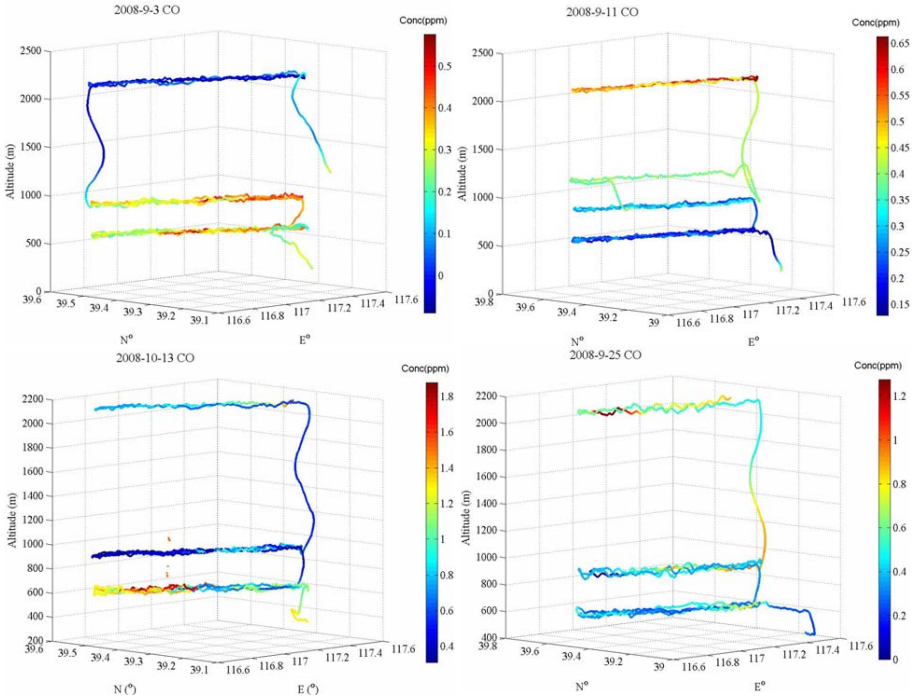

Fig. 6. Variation of CO concentration at different heights in different flights.

ACPD
13, 2877–2912, 2013

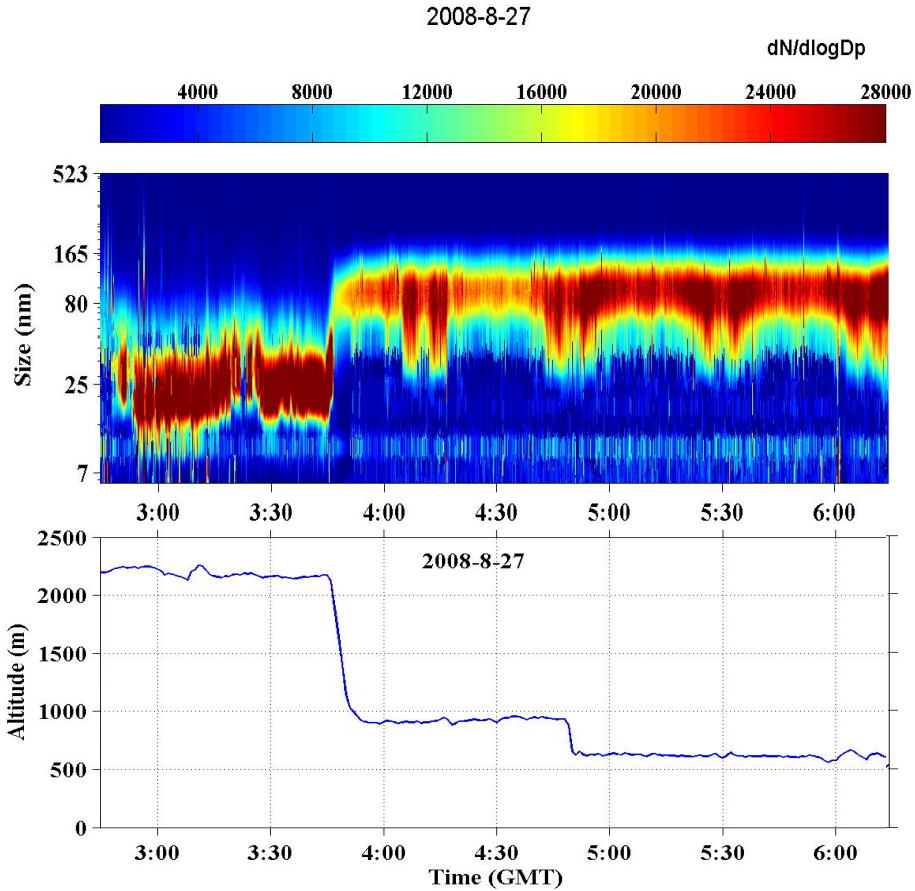

Fig. 7. Variation of size distributions for 5.6–560 nm range with altitudes at different heights on 27 August flight.

ACPD
13, 2877–2912, 2013

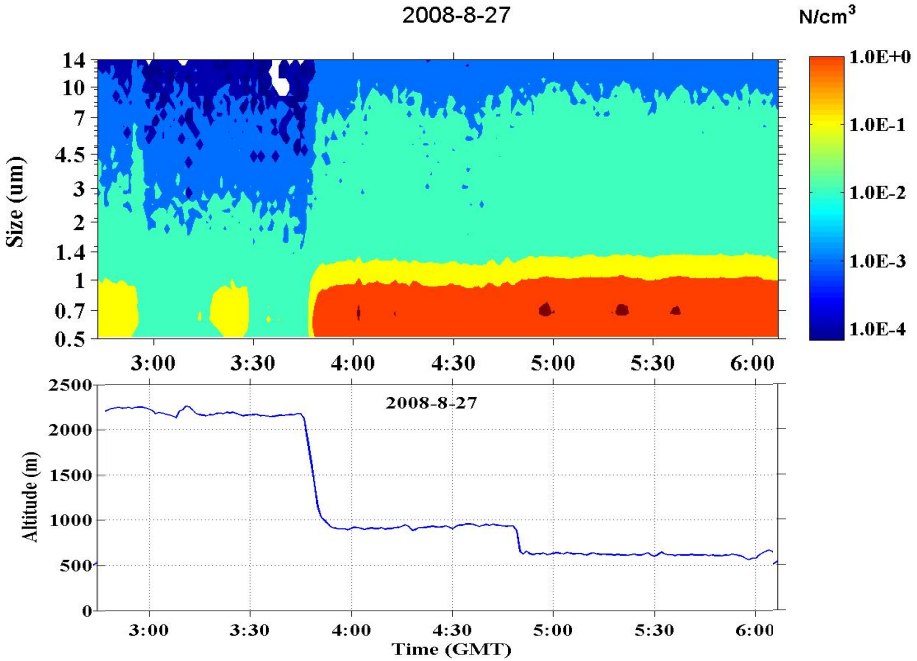

Fig. 8. Variation of size distributions for 0.5–20 μm range with altitudes at different heights on 27 August flight.

ACPD
13, 2877–2912, 2013

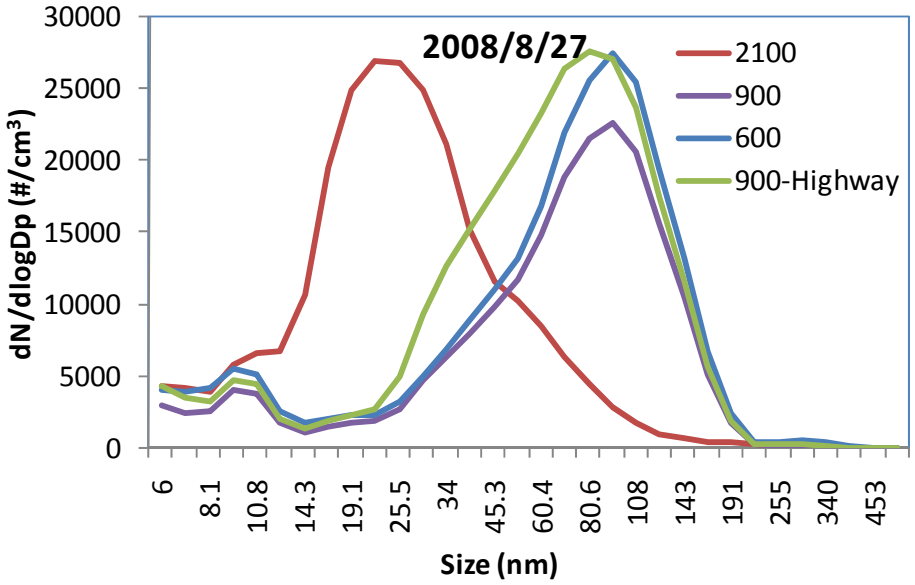

Fig. 9. The average size distribution of 5.6–560 nm particles at different heights on 27 August flight.

ACPD
13, 2877–2912, 2013